

# Numerical Heat Transfer, Part B: Fundamentals

## An International Journal of Computation and Methodology

ISSN: (Print) (Online) Journal homepage: [www.tandfonline.com/journals/unhb20](http://www.tandfonline.com/journals/unhb20)

# Thermal and solutal stratified Heimanz flow of AA7072-deionized water over a wedge in the presence of bioconvection

Shuguang Li, V. Puneeth, Fuad A. M. Al-Yarimi, S. Manjunatha, M. Shoaib Anwar & Ali J. Chamkha

To cite this article: Shuguang Li, V. Puneeth, Fuad A. M. Al-Yarimi, S. Manjunatha, M. Shoaib Anwar & Ali J. Chamkha (07 Mar 2024): Thermal and solutal stratified Heimanz flow of AA7072-deionized water over a wedge in the presence of bioconvection, Numerical Heat Transfer, Part B: Fundamentals, DOI: [10.1080/10407790.2024.2319337](https://doi.org/10.1080/10407790.2024.2319337)

To link to this article: <https://doi.org/10.1080/10407790.2024.2319337>



Published online: 07 Mar 2024.



Submit your article to this journal [↗](#)



Article views: 16





View related articles [↗](#)



View Crossmark data [↗](#)



# Thermal and solutal stratified Heimanz flow of AA7072-deionized water over a wedge in the presence of bioconvection

Shuguang Li<sup>a</sup>, V. Puneeth<sup>b</sup> , Fuad A. M. Al-Yarimi<sup>c</sup>, S. Manjunatha<sup>d</sup>,  
M. Shoaib Anwar<sup>e</sup>, and Ali J. Chamkha<sup>f</sup> 

<sup>a</sup>School of Computer Science and Technology, Shandong Technology and Business University, Yantai, P.R. China; <sup>b</sup>Centre for Mathematical Needs, Department of Mathematics, CHRIST (Deemed to be University), Bengaluru, India; <sup>c</sup>Department of Computer Science, King Khalid University, Abha, Saudi Arabia; <sup>d</sup>Department of Sciences and Humanities, CHRIST (Deemed to be University), Bangalore, India; <sup>e</sup>Department of Mathematics, University of Jhang, Jhang, Pakistan; <sup>f</sup>Faculty of Engineering, Kuwait College of Engineering, Doha, Kuwait

## ABSTRACT

The bioconvective Heimanz flow of nanofluid across a wedge with thermal stratification is analyzed in this article. The wedges are often seen in glider aircraft, rocket climbing frames, etc. The nanofluid considered in this study is composed of aluminum alloys of AA7072 and deionized water. The AA7072 alloys are specially manufactured materials composed of Aluminum and Zinc in the ratio of 98 : 1 along with metals like silicon, ferrous, and copper so that they possess enhanced heat transfer features. The mathematical model is formed using the modified Buongiorno's model that includes the discussions related to slip mechanisms and volumetric analysis in terms of the weight of the nanoparticle. The model is in the form of partial differential equations and is later converted to ordinary differential equations with the assistance of similarity transformation. This set of equations is solved by the Differential Transformation Method (DTM) and the outcomes are discussed through graphs. ,

## ARTICLE HISTORY

Received 23 June 2023  
Revised 19 September 2023  
Accepted 26 January 2024

## KEYWORDS

Bioconvection; Buongiorno's model; Heimanz flow; modified differential transform method; thermal stratification; wedge

## 1. Introduction

The small dimensions and huge specific areas of nanoparticles offer enhanced thermophysical properties. This enables its usefulness in various technological aspects including nanotechnology and microelectromechanical systems (MEMS). It is quite a well-known fact that the thermal properties of metals are far better than that of traditional fluids like water, propylene glycol, etc. Thus, fluids with solid particle dispersion are a very effective tool for heat transfer in appliances like engine cooling, refrigeration, solar water heaters, thermal storage, etc. In this regard, Li et al. [1] accustomed the Cattaneo heat flux form to discuss the stagnation point flow of nanofluid. Khan et al. [2] discussed the friction drag that occurs in the flow of water suspended by carbon nanotubes (CNTs). Nadeem et al. [3] analyzed the flow behavior of nanofluid flowing past an oscillatory stretching sheet. The impact of mixed convection for the flow of non-Newtonian type nanofluid was examined by Qaiser et al. [4] by considering Walter's-B nanofluid model. Similarly, Khan et al. [5] discussed mixed convection for the flow of water combined with  $SiO_2$  and  $Al_2O_3$ . Nadeem et al. [6] analyzed the flow behavior of viscous nanofluid flowing over a

### Nomenclature

$\alpha$	Thermal Diffusivity ( $m^2s^{-1}$ )	$N_w$	Motile density at the wall
$\gamma$	Wedge angle	$Nb$	Dimensionless Brownian motion
$\kappa$	Thermal conductivity ( $Wm^{-1}K^{-1}$ )	$Nt$	Dimensionless thermophoresis
$\Lambda$	velocity ratio	$Nu_x$	Nusselt number
$\mu$	Dynamic viscosity ( $kgm^{-1}s^{-1}$ )	$Pe$	Peclet number
$\nu$	Kinematic viscosity ( $m^2s^{-1}$ )	$Pr$	Prandtl number
$\Omega$	Motile density difference parameter	$q_r$	Thermal radiation
$\psi$	Stream function	$S_1, S_2$	Stratification parameters
$\rho$	Density ( $kgm^{-3}$ )	$Sb$	Bioconvection Schmidt number
$(u, v)$	Velocity components ( $ms^{-1}$ )	$Sc$	Schmidt number
$C$	Concentration ( $mol$ )	$Sc$	Schmidt number
$C_\infty$	Ambient Mass concentration	$Sh_x, Nn_x$	Sherwood numbers
$C_w$	Mass concentration at the wall	$T$	Temperature ( $K$ )
$Cf_x$	Skin friction co-efficient	$T_\infty$	Ambient Temperature
$Cp$	Specific heat capacity ( $Jkg^{-1}K^{-1}$ )	$T_w$	Temperature at the wall
$D_B$	Brownian motion diffusivity	$f$	Fluid
$D_T$	Thermophoresis Diffusivity	$nf$	Nanofluid
$N$	Motile density	$s$	Nanoparticle
$N_\infty$	Ambient motile density		

curved surface. Barnoon et al. [7] discussed entropy generation for various nanofluids flowing between two horizontal concentric pipes. Al-Farhany et al. [8] created a model to study the double-diffusive convection in the fluid flowing in a curvilinear cavity. Hymavathi and Sridhar [9] discussed the heat and mass transfer of Casson nanofluid considering the impact of suction on the surface. Sridhar et al. [10] studied the flow of Williamson nanofluid considering the surface to be a permeable sheet having irregular thickness. Javed et al. [11] studied the impingement of fluid and its thermal characteristics while the fluid is obliquely flowing on the sheet. Usafzai et al. [12] studied the jet flow past a wall considering the radiation effect.

In studies related to the volumetric analysis of nanofluid, the velocity slip between fluid and nanoparticles is ignored. Further, uniform nanoparticle concentration is assumed which is practically not possible to achieve. The nanoparticles suspended in the fluid experience certain slip mechanisms among which thermophoresis and Brownian motion have a prominent role. Hence, modified Buongiorno's model has been incorporated in this volumetric analysis of nanofluid flow that includes the weight of the nanoparticle suspension and slip mechanisms discussed by Buongiorno [13]. In this regard, many researchers have worked on analyzing the effect of thermophoresis and Brownian motion. Eslamian et al. [14] discussed the Brownian motion and thermophoresis in the convective flow of a nanofluid in a porous channel. Matin and Ghanbari [15] showed that the Brownian motion and thermophoresis enhance the heat transfer rate. These slip mechanisms were compared for three different nanofluids by Haddad et al. [16]. The flow of Casson nanofluid [17], micropolar nanofluid [18,19] under the influence of Brownian motion and thermophoresis has been discussed using Buongiorno's model. Sangeetha and De [20] discussed the significance of thermophoresis and Brownian motion considering the buoyancy effects for the free stream flow. Furthermore they [21,22] have also studied these effects on the Maxwell and Casson nanofluid considering the porous medium. Also, in their extensive study on these impacts, they considered the aspect of activation energy and binary chemical reaction influence over the heat mass transfer in nanofluid. Iqbal et al. [23] studied these effects considering the radiation impact on the Heilmann flow. Xin et al. [24] implemented Thompson and Troian slips at the boundary to analyze the thermal characteristics of Williamson nanofluid in the presence of slip mechanisms. Rehman et al. [25] further explained the Williamson model using the Darcy–Frochheimer model. More studies on the heat transfer properties of nanofluid can be seen in [26–30].

The phenomenon of random movement of microorganisms leads to bioconvection. These microbes may move as a single cell or as a colony of cells. The process of bioconvection occurs when the microbes settle in the upper fluid region because in the lower layers of fluid will have an irregular density distribution. Once the fluid layers at the lower regions become less dense than the upper fluid, the microbes tend to move downwards therefore convective instability occurs and patterns of convection are observed [31]. These motions of microbes are self-actuated and hence they are called self-propelled microorganisms. The swimming orientation of microorganisms is governed by the action of their flagella. Numerous other factors that may influence the direction of swimming include gravity, concentration, stress intensity, and vortices. Based on these factors, the microorganisms are classified into various classes. In this research, gyrotactic microorganisms are considered that move around due to concentration gradient and are useful for agricultural, chemical, and environment-friendly products like fuels, gasoline, and fertilizers. Even though the nanoparticles suspension in base fluid enhances the thermal conductivity, there are warnings of inadequate mixing [32]. This is sorted out by the swimming of microorganisms as they help in avoiding the agglomeration of nanoparticles that eventually occurs in the nanofluid flow and safeguards the appliances [33]. In this regard, Chu et al. [34] examined the effect of nonlinear thermal radiation on the flow of nanofluid past a rotating surface in the presence of microorganisms. An enhancement in thermal conduction due to the presence of microorganisms was observed by Islam et al. [35]. Khan et al. [36] discussed the entropy generation in the presence of gyrotactic microorganisms within the Oldroyd-B nanofluid using the Cattaneo-Christov model. Waqas et al. [37] measured the swimming of microorganisms in the flow of viscous nanofluid. Reddy et al. [38] performed numerical analysis to study the impact of the magnetic field on the Eyring-Powell nanofluid considering the impact of the microorganisms.

In recent times, various nanomaterials have been discovered and among these nanomaterials, aluminum alloy (AA7072) is a special variant that has better chemical and physical properties. These alloys of aluminum have an important role to play in the industries related to aerospace, specifically in the fabrication of appliances like glider aircraft, rocket climbing frames, etc. From the above literature survey, it was observed that the works related to the analysis of nanoparticle weight on the bioconvective flow are rarely available. Thus, this article reports the first study that analyses the influence of the weight of nanoparticles in the flow of nanofluid past a wedge. The major objective of this study is to design a mathematical model that includes the impact of physical scenarios such as thermophoresis and Brownian motion on the nanofluid flowing past a wedge. These forces arise naturally due to the motion of the solid particles. Along with this objective, it is also aimed to provide a strong method of solution to the differential equations describing the flow. The nanofluid considered here is composed of AA7072 and deionized water. The solution for the mathematical model that describes the flow is obtained through the Differential Transformation method (DTM) and Padé approximant. The effects of various parameters involved in the study are interpreted graphically. The process involved in the research process is indicated through the flow chart (Figure 1).

## 2. Mathematical model

A steady two-dimensional laminar flow of AA7072– deionized water is considered across a wedge in the existence of gyrotactic microorganisms. The nanoparticle concentration is assumed to be diluted so that it has no effect on the swimming of microorganisms. Further, the movement of the nanoparticle within the fluid experiences thermophoresis and Brownian motion hence these phenomena are incorporated in the model so as to attain better results that are best suited to the practical scenario. The modified Buongiorno model has been incorporated to analyze the effects of these slip mechanisms along with the volumetric analysis. The flow geometry is described using Cartesian coordinates (Figure 2) and the system is surrounded with temperature  $T_\infty$ ,

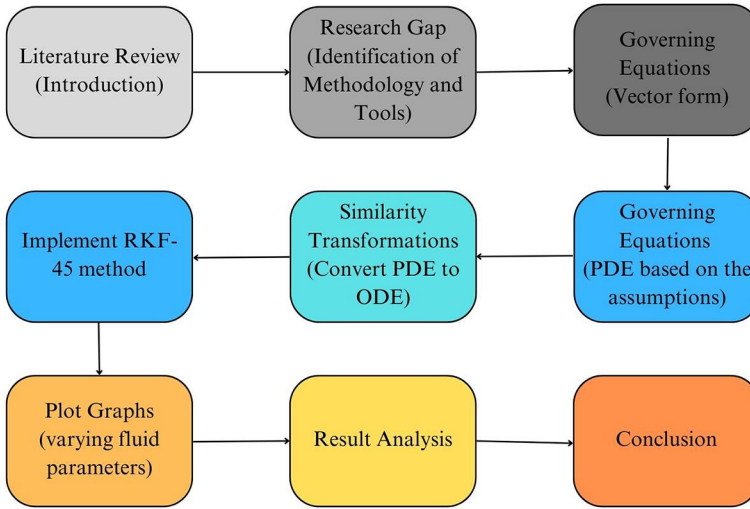


Figure 1. Flow chart of the research process.

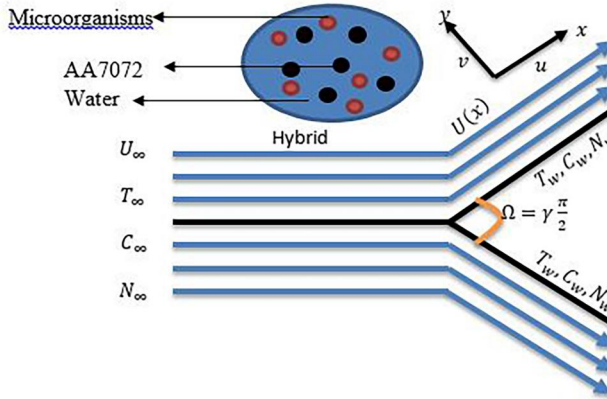


Figure 2. Flow geometry.

nanoparticle concentration  $C_\infty'$  and motile density  $N_\infty$ . The system is configured with the surface temperature  $T_w$ , nanoparticle concentration  $C_w$ , and motile density  $N_w$ . The wedge is assumed to move with the free stream velocity  $U_\infty$ . The basic governing equations of the flow in the vector form are given by:

$$\begin{aligned}
 \nabla \cdot \vec{q} &= 0 \\
 (\vec{q} \cdot \nabla) \vec{q} &= \frac{\mu_{nf}}{\rho_{nf}} \nabla^2 \vec{q} \\
 (\vec{q} \cdot \nabla) T &= \alpha_{nf} \nabla^2 T \\
 (\vec{q} \cdot \nabla) C &= D_B \nabla^2 C \\
 (\vec{q} \cdot \nabla) N &= D_N \nabla^2 N
 \end{aligned}$$

Upon incorporating the assumptions in the above equations, the resulting mathematical model will be of the form [39,40]:

$$\frac{\partial u}{\partial x} + \frac{\partial v}{\partial y} = 0 \tag{1}$$

$$u \frac{\partial u}{\partial x} + v \frac{\partial u}{\partial y} = U \frac{\partial U}{\partial x} + \frac{\mu_{nf}}{\rho_{nf}} \frac{\partial^2 u}{\partial y^2} \quad (2)$$

$$u \frac{\partial T}{\partial x} + v \frac{\partial T}{\partial y} = \alpha_{nf} \frac{\partial^2 T}{\partial y^2} + \frac{(\rho C_p)_{nf}}{(\rho C_p)_f} \left[ \frac{D_B}{C_\infty} \frac{\partial T}{\partial y} \frac{\partial C}{\partial y} + \frac{D_T}{T_\infty} \left( \frac{\partial T}{\partial y} \right)^2 \right] \quad (3)$$

$$u \frac{\partial C}{\partial x} + v \frac{\partial C}{\partial y} = D_B \frac{\partial^2 C}{\partial y^2} + \frac{D_T C_\infty}{T_\infty} \frac{\partial^2 T}{\partial y^2} \quad (4)$$

$$u \frac{\partial N}{\partial x} + v \frac{\partial N}{\partial y} = D_N \frac{\partial^2 N}{\partial y^2} - \frac{bW_c}{C_w - C_\infty} \left[ \frac{\partial}{\partial y} \left( N \frac{\partial C}{\partial y} \right) \right] \quad (5)$$

Subjected to the following Stratification conditions [41]:

$$\begin{aligned} u = U_w, \quad v = 0, \quad T = T_w = T_0 + b_1 x, \quad C = C_w = C_0 + c_1 x, \quad N = N_w \quad \text{at } y = 0 \\ u \rightarrow U, \quad T \rightarrow T_\infty = T_0 + b_2 x, \quad C \rightarrow C_\infty = C_0 + c_2 x, \quad N \rightarrow N_\infty \quad \text{as } y \rightarrow \infty \end{aligned} \quad (6)$$

The thermophysical constants of deionized water and AA7072 aluminum alloy are specified in Table 1 and the thermophysical parameters of the nanofluid like  $\rho_{nf}$ ,  $\kappa_{nf}$ ,  $(Cp)_{nf}$  and  $\phi$  are defined as:

$$\begin{aligned} \phi &= \frac{\frac{w_s}{\rho_s}}{\frac{w_s}{\rho_s} + \frac{w_f}{\rho_f}}, & \frac{\mu_{nf}}{\mu_f} &= \frac{1}{(1 - \phi)^{2.5}}, & \frac{\rho_{nf}}{\rho_f} &= 1 - \phi + \phi \frac{\rho_s}{\rho_f}, \\ \frac{(\rho Cp)_{nf}}{(\rho Cp)_f} &= 1 - \phi + \phi \frac{(\rho Cp)_s}{(\rho Cp)_f}, & \frac{\kappa_{nf}}{\kappa_f} &= \frac{1 - \phi + 2\phi \left( \frac{\kappa_s}{\kappa_s - \kappa_f} \right) \log n \left( \frac{\kappa_s}{\kappa_s - \kappa_f} \right)}{1 - \phi + 2\phi \left( \frac{\kappa_f}{\kappa_s - \kappa_f} \right) \log n \left( \frac{\kappa_s}{\kappa_s - \kappa_f} \right)} \end{aligned}$$

The following similarity transformations are used to non-dimensionalise Eqs. (2)–(5):

$$\begin{aligned} \psi(\eta) &= \sqrt{\frac{2\nu_f x U}{1 + \beta}} \bar{F}(\eta), & \bar{\theta}(\eta) &= \frac{T - T_\infty}{T_w - T_\infty}, & \bar{P}(\eta) &= \frac{C - C_\infty}{C_w - C_\infty}, & \bar{X}(\eta) &= \frac{N - N_\infty}{N_w - N_\infty}, \\ \eta &= \sqrt{\frac{(1 + \beta)U}{2\nu_f x}} \end{aligned} \quad (7)$$

By making use of Eq. (7), the continuity Eq. (1) is satisfied and remaining Eqs. (2)–(5) can be written as:

$$\frac{\mu_{nf}}{\mu_f} \bar{F}''' - \frac{\rho_{nf}}{\rho_f} \bar{F} \bar{F}'' + \frac{\rho_{nf}}{\rho_f} \gamma (1 - \bar{F}'^2) = 0 \quad (8)$$

$$\frac{\kappa_{nf}}{\kappa_f} \bar{\theta}'' + \frac{(\rho Cp)_{nf}}{(\rho Cp)_f} [Pr \bar{F} \bar{\theta}' + Nb \bar{\theta}' \bar{P}' + Nt \bar{\theta}'^2] = 0 \quad (9)$$

$$\bar{P}'' + Sc \bar{F} \bar{P}' + \frac{Nt}{Nb} \bar{\theta}'' = 0 \quad (10)$$

**Table 1.** Thermophysical constants of AA7072 and deionized water.

Properties	AA7072	Deionized water
Density	2720	997.2
Thermal conductivity	222	0.579
Heat capacity	893	4221

$$\bar{X}'' + Sb\bar{F}\bar{X}' - Pe(\bar{X}\bar{P}'' + \bar{X}'\bar{P}' + \Omega\bar{P}'') = 0 \quad (11)$$

The boundary conditions corresponding to (6) are reduced to:

$$\begin{aligned} \bar{F} = 0, \quad \bar{F}' = \Lambda, \quad \bar{\theta} = 1 - S_1, \quad \bar{P} = 1 - S_2, \quad \bar{X} = 1 \quad \text{at} \quad \eta = 0 \\ \bar{F}' \rightarrow 1, \quad \bar{\theta} \rightarrow 0, \quad \bar{P} \rightarrow 0, \quad \bar{X} \rightarrow 0 \quad \text{as} \quad \eta \rightarrow \infty \end{aligned} \quad (12)$$

$\gamma$  determines the wedge angle. If  $\gamma = 0$  then the wedge acts as a flat plate and  $\gamma = 1$  describes the wedge half-angle  $90^\circ$ . The case  $\gamma = 1$  is a 2-D stagnation point flow also called Heimanz flow. The skin friction coefficient, local Nusselt number, local Sherwood number and local motile density number are defined as:

$$\begin{aligned} Cf_x = \frac{\mu_{nf} \frac{\partial u}{\partial y}_{y=0}}{\rho_f U_w^2}, \quad Nu_x = -x \frac{\kappa_{nf} \frac{\partial T}{\partial y}_{y=0}}{\kappa_f (T_w - T_\infty)}, \quad Sh_x = -xD_B \frac{\frac{\partial C}{\partial y}_{y=0}}{D_B (C_w - C_\infty)}, \\ Nn_x = -xD_N \frac{\frac{\partial N}{\partial y}_{y=0}}{D_N (N_w - N_\infty)} \end{aligned} \quad (13)$$

By incorporating (7) in (13), the following relations are obtained:

$$\begin{aligned} \sqrt{\frac{2Re_x}{\beta+1}} Cf = \frac{\bar{F}''(0)}{(1-\phi)^{2.5}}, \quad \sqrt{\frac{2}{(\beta+1)Re_x}} Nu_x = -\frac{\kappa_{nf}}{\kappa_f} \bar{\theta}'(0), \\ \sqrt{\frac{2}{(\beta+1)Re_x}} Sh_x = -D_B \bar{P}'(0), \quad \sqrt{\frac{2}{(\beta+1)Re_x}} Nn_x = -D_N \bar{X}'(0) \end{aligned} \quad (14)$$

The nondimensional parameters involved in the system are defined as:

$$\begin{aligned} Pr = \frac{\alpha_f}{\nu_f}, \quad Nt = \frac{\tau D_T (T_w - T_\infty)}{\alpha_f T_\infty}, \quad Nb = \frac{\tau D_B (C_w - C_\infty)}{\alpha_f C_\infty}, \quad \Lambda = \frac{U_w}{U_\infty}, \\ S_1 = \frac{b_2}{b_1}, \quad S_2 = \frac{c_2}{c_1}, \quad Re_x = \frac{Ux}{\nu_f}, \quad Pe = \frac{bW_c}{D_N}, \quad Sc = \frac{\nu_f}{D_B}, \quad Sb = \frac{\nu_f}{D_N}, \quad \gamma = \frac{2\beta}{\beta+1} \end{aligned}$$

### 3. Solution methodology

The transformed system of ordinary differential equations (8)–(11) along with the boundary condition (12) are solved using DTM as described below.

#### 3.1. Introduction to differential transformation method (DTM)

Among the various methods that are available to solve nonlinear ordinary differential equations DTM is being widely used by researchers and academicians for various advantages it possesses [42–45]. It is a semi-analytical method i.e. it has both numerical and analytical approaches for solving the system of differential equations. For a given differential equation, it generates a polynomial solution that requires symbolic computations. The traditional Taylor series method is computationally challenging for the users and takes a longer time whereas DTM follows an iterative process to obtain the solution for Taylor series solution of differential equations. The major benefit of this technique is that it can be used directly for both linear and nonlinear differential equations without any linearization or perturbation techniques. Another prominent advantage is that it is capable of reducing the size of computational work while still providing accurate solutions with a fast convergence rate. The basic definitions and transformations related to DTM are introduced in [46]. Some of the major theorems corresponding to DTM are [47,48]:

**Theorem 1.** The transformation  $\mathcal{L}(j) = \mathcal{L}_1(j) \pm \mathcal{L}_2(j)$  if the function is of the form  $L(z) = L_1(z) \pm L_2(z)$ .

**Theorem 2.** The transformation  $\mathcal{L}(j) = \alpha_1 \mathcal{L}_1(j)$  for the function  $L(z) = \alpha_1 L_1(z)$ .

**Theorem 3.** The transformation  $\mathcal{L}(j) = \frac{(j+m)!}{j!} \mathcal{L}_1(j+m)$  for the function  $L(z) = \frac{d^m L_1(z)}{dz^m}$ .

**Theorem 4.** The transformation  $\mathcal{L}(j) = \sum_{j_1=0}^j \mathcal{L}_1(j_1) \mathcal{L}_2(j-j_1)$  for the product  $L(z) = L_1(z)L_2(z)$ .

**Theorem 5.** If  $L(z) = z^m$ , then the transformation of  $L(z)$  is given by  $\mathcal{L}(j) = \delta(j-m) = \begin{cases} 1 & j = m \\ 0 & j \neq m \end{cases}$

Using the above definitions and theorems, the nondimensional system of differential equations (8)–(12) are converted to power series as shown below:

$$F[L+3] = \frac{\mu_f \rho_{nf}}{\mu_{nf} \rho_f} \frac{L!}{(L+3)!} \left[ \sum_{b=0}^L (b+1)(b+2)F[L-b]F[b+2] - \frac{2\beta}{\beta+1} \sum_{b=0}^L \delta[L-b] + \frac{2\beta}{\beta+1} \sum_{b=0}^L (L-b+1)(b+1)F[L-b+1]F[b+1] \right] \quad (15)$$

$$\theta[L+2] = -\frac{L!}{(L+2)!} \frac{\kappa_f}{\kappa_{nf}} \left[ \frac{(\rho Cp)_{nf}}{(\rho Cp)_f} Pr \sum_{b=0}^L (b+1)F[L-b]\theta[b+1] + Nb \sum_{b=0}^L (L-b+1)(b+1)\theta[L-b+1]P[b+1] + Nt \sum_{b=0}^L (L-b+1)(b+1)\theta[L-b+1]\theta[b+1] \right] \quad (16)$$

$$P[L+2] = -\frac{L!}{(L+2)!} \left[ \frac{Nt}{Nb} (L+1)(L+2)\theta[j+2] + Sc \sum_{b=0}^L (b+1)P[b+1]F[L-b] \right] \quad (17)$$

$$X[L+2] = -\frac{L!}{(L+2)!} \left[ Sb \sum_{b=0}^L (b+1)X[b+1]F[L-b] - Pe \left( \sum_{b=0}^i (b+1)(L-b+1)X[b+1]P[L-b+1] + \sum_{b=0}^L (b+1)(b+2)P[b+2]X[L-b] + \Omega(L+1)(L+2)P[L+2] \right) \right] \quad (18)$$

The constants that are accompanied by the system of Eqs. (15)–(18) are as follows:

$$\begin{aligned} F[0] &= 0, & F[1] &= \Lambda, & F[2] &= g_1, & \Theta[0] &= 1 - S_1, & \Theta[1] &= g_2, \\ \Phi[0] &= 1 - S_2, & \Phi[1] &= g_3, & X[0] &= 1, & X[1] &= g_4 \end{aligned} \quad (19)$$

### 3.2. Padé approximation

The convergence radius of the power series  $\mathcal{C}(x) = \sum_{i=0}^{\infty} \alpha_i x^i$  ought not be broad enough and hence, polynomials are chosen for obtaining approximations. The power series gets transformed into a rational function because of the Padé approximant and the rational function obtained is of the form:

$$\left[ \frac{c}{b} \right] = \frac{\mathcal{A}_c(x)}{\mathcal{B}_d(x)} \quad (20)$$

**Table 2.** Comparison of the result with the existing literature.

m	$\phi$	$-F''(0)$			$-\theta'(0)$		
		[50]	[51]	This study	[50]	[51]	This study
0	0.1	0.6169	0.616929	0.616928	1.0189	1.018845	1.018905
	0.2	0.7978	0.797872	0.797871	1.1561	1.156053	1.156055
0.5	0.1	1.3648	1.364842	1.364842	1.2460	1.246064	1.246064
	0.2	1.7655	1.765142	1.765541	1.4082	1.408206	1.408206
1	0.1	1.6192	1.619291	1.619291	1.3010	1.301085	1.301088
	0.2	2.0942	2.094220	2.094220	1.4691	1.469032	1.469033

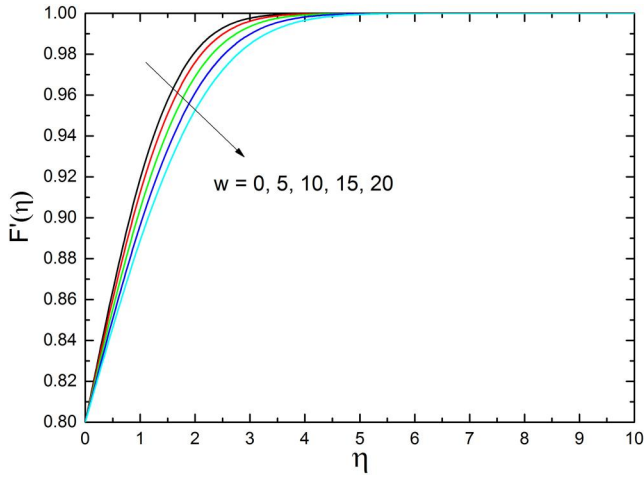


**Figure 3.** Impact of  $w$  on  $F'(\eta)$ .

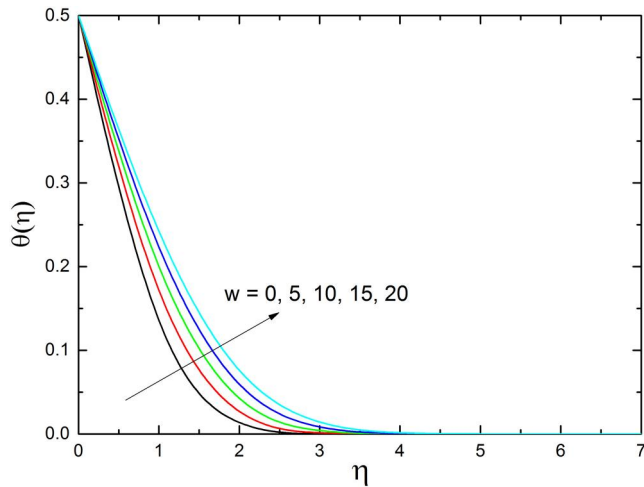


**Figure 4.** Impact of  $w$  on  $\Theta(\eta)$ .

where the polynomials  $\mathcal{A}_c(x)$  and  $\mathcal{B}_d(x)$  are of degree at most  $c$  and  $d$ , respectively. On expanding  $\mathcal{C}(x)$ , the fraction (20) looks like

$$\frac{\mathcal{A}_c(x)}{\mathcal{B}_d(x)} = \frac{\mathcal{A}_0 + \mathcal{A}_1x + \mathcal{A}_2x^2 + \mathcal{A}_3x^3 + \dots + \mathcal{A}_cx^c}{\mathcal{B}_0 + \mathcal{B}_1x + \mathcal{B}_2x^2 + \mathcal{B}_3x^3 + \dots + \mathcal{B}_dx^d} \tag{21}$$

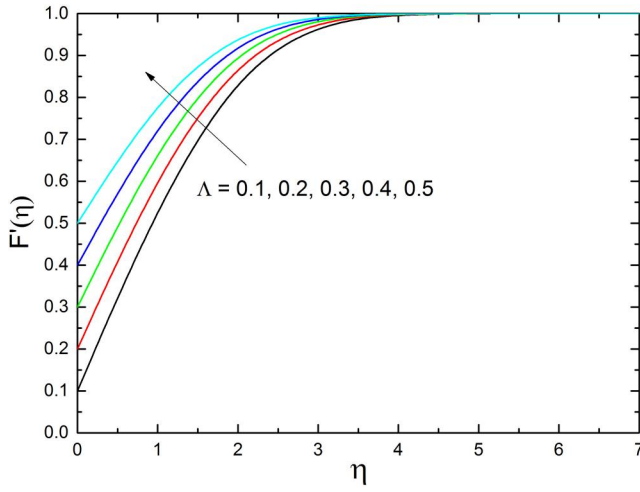


Figure 5. Impact of  $\Lambda$  on  $F'(\eta)$ .

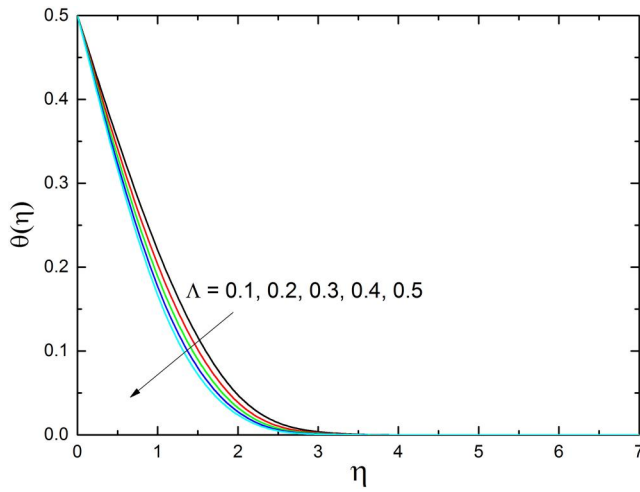


Figure 6. Impact of  $\Lambda$  on  $\Theta(\eta)$ .

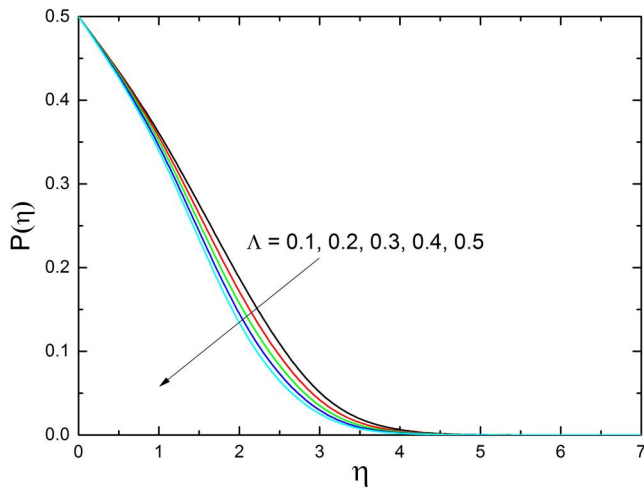


Figure 7. Impact of  $\Lambda$  on  $P(\eta)$ .

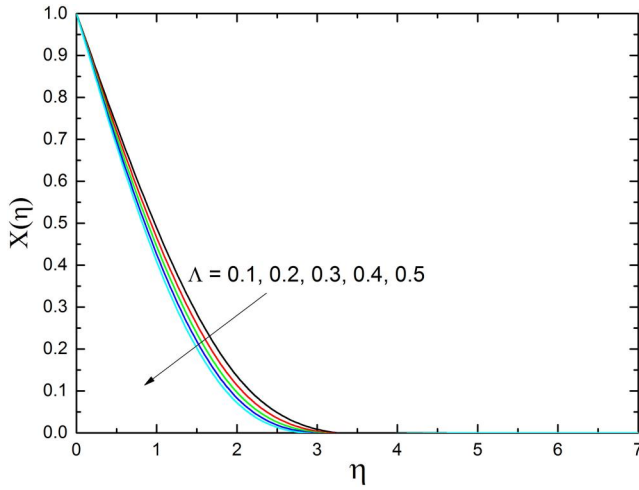


Figure 8. Impact of  $\Lambda$  on  $X(\eta)$ .

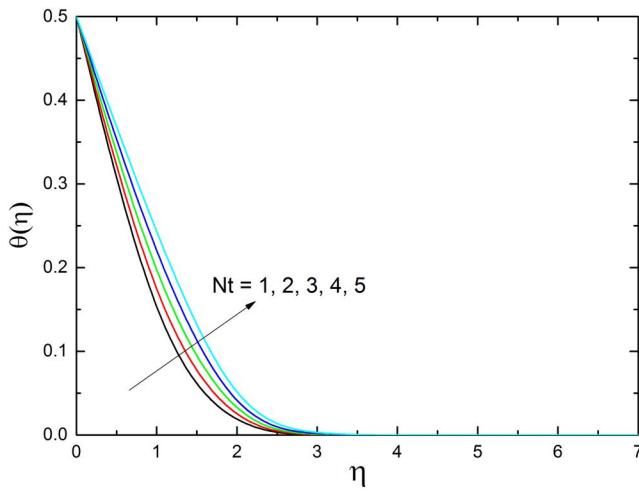


Figure 9. Impact of  $Nt$  on  $\Theta(\eta)$ .

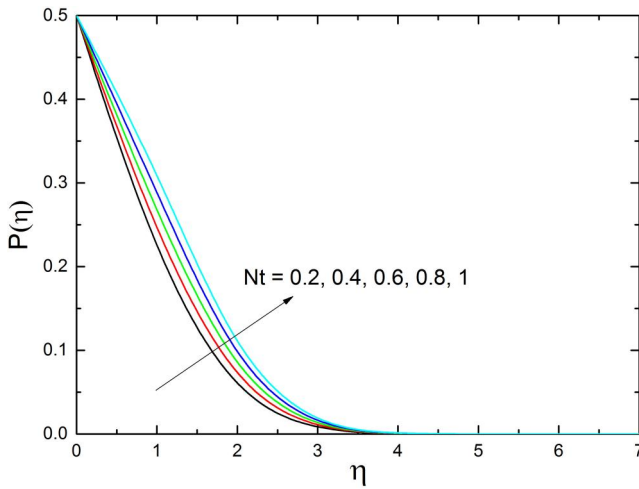


Figure 10. Impact of  $Nt$  on  $P(\eta)$ .

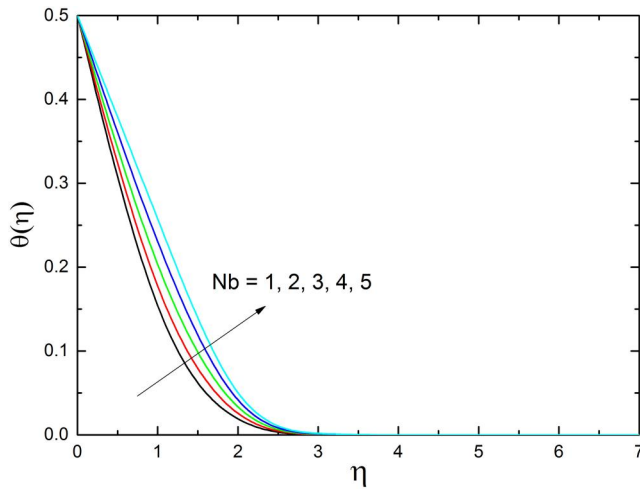


Figure 11. Impact of  $Nb$  on  $\Theta(\eta)$ .

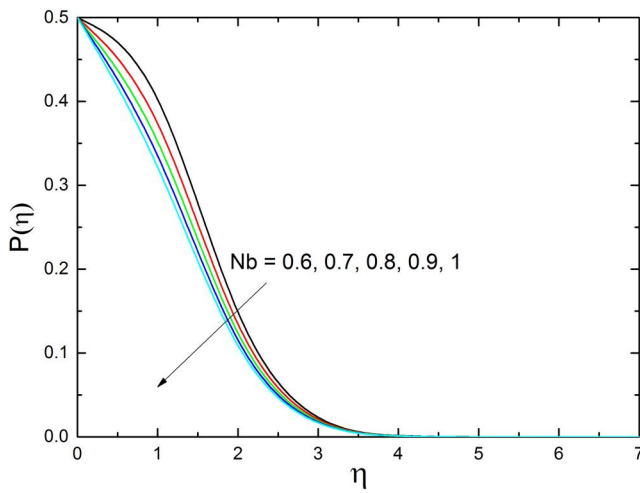


Figure 12. Impact of  $Nb$  on  $P(\eta)$ .

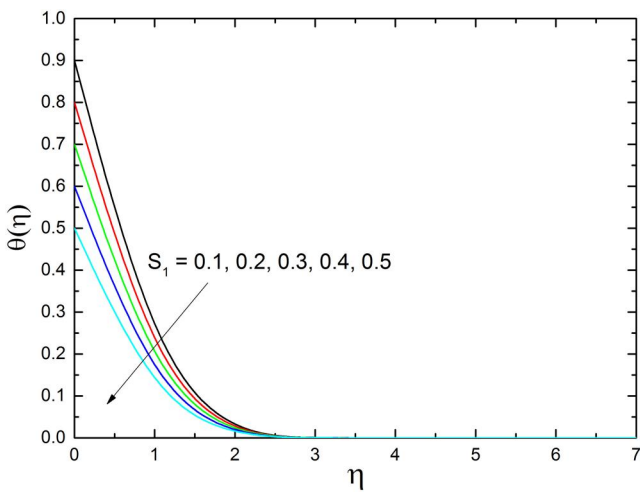


Figure 13. Impact of  $S_1$  on  $\Theta(\eta)$ .

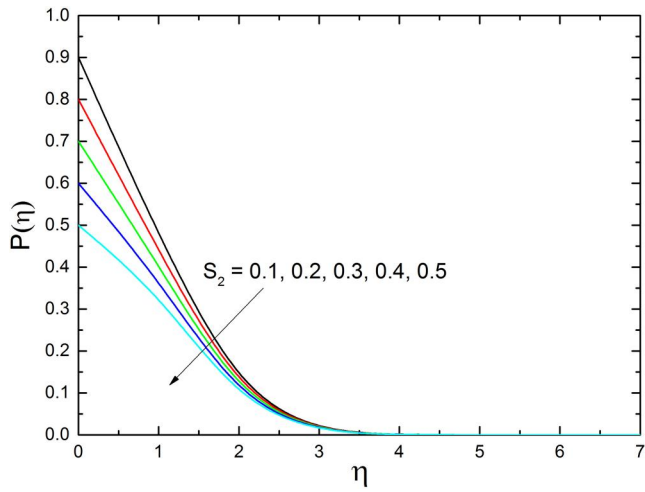


Figure 14. Impact of  $S_2$  on  $P(\eta)$ .

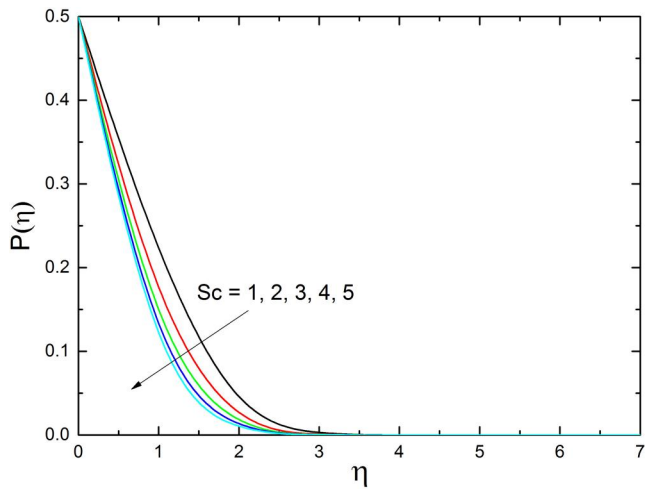


Figure 15. Impact of  $Sc$  on  $P(\eta)$ .

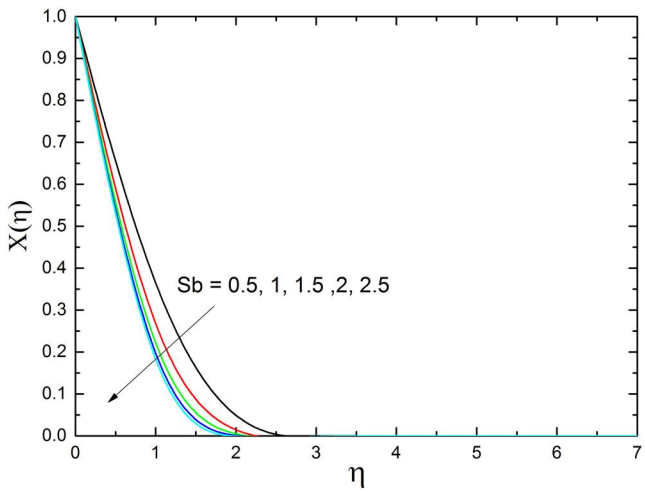


Figure 16. Impact of  $S_b$  on  $X(\eta)$ .

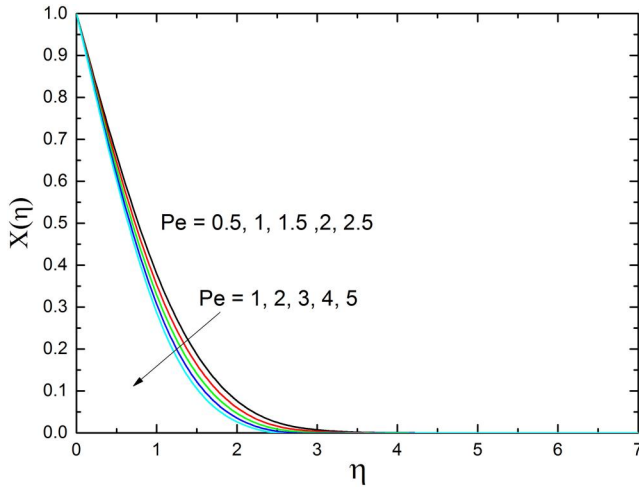


Figure 17. Impact of  $Pe$  on  $X(\eta)$ .

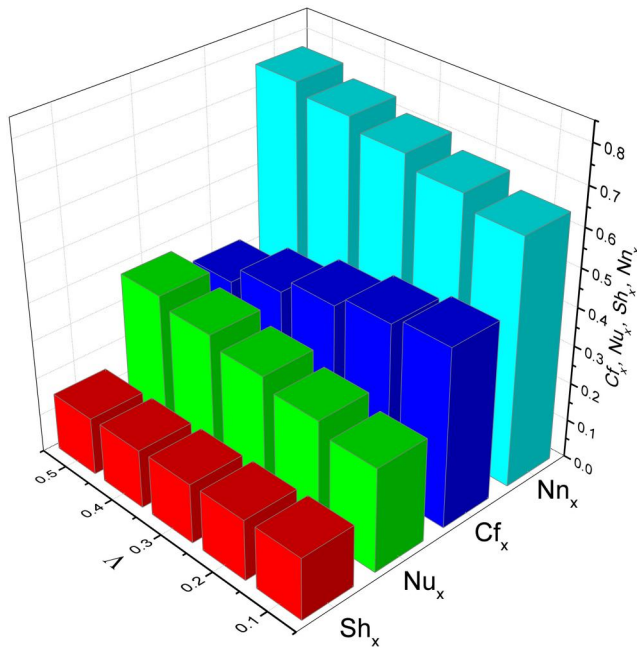


Figure 18. Impact of  $\Lambda$  on  $Cf_x$ ,  $Nu_x$ ,  $Sh_x$  &  $Nn_x$ .

The normalizing condition  $\mathcal{B}_n(0) = 1$  is applied to the above equation. The numerator and denominator, respectively, have  $c + 1$  and  $d$  independent coefficients, as seen in the above fraction. The most significant disadvantage of using the padé approximant is determining  $[c, d]$  to get the best outcome. The approximants  $[c, d]$  are entirely created using the algebraic procedures [46]. These two values were chosen to be equivalent in this investigation. The DTM solution may or may not fulfill the infinite boundary conditions [49]. As a result, when the series solution is combined with the Padé approximant, the boundary value problem on infinite domains is solved more effectively. Equations (15)–(18) are thus subjected to Padé Approximants around  $x = 0$ , as

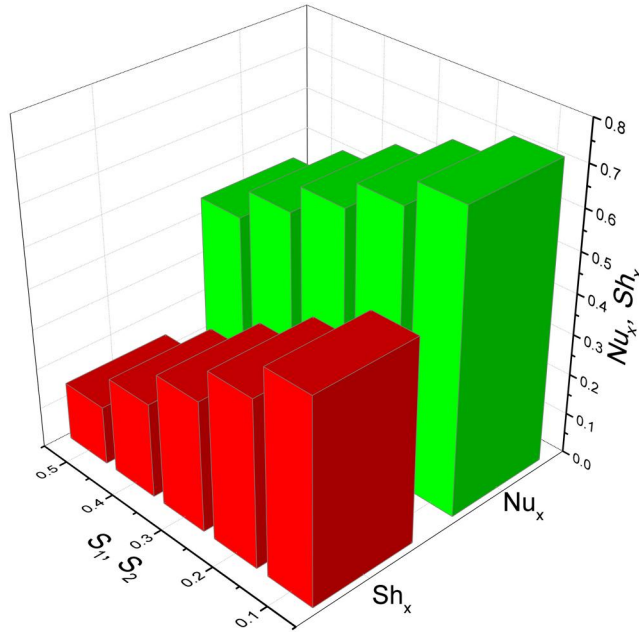


Figure 19. Impact of  $S_1$  &  $S_2$  on  $Nu_x$  &  $Sh_x$ .

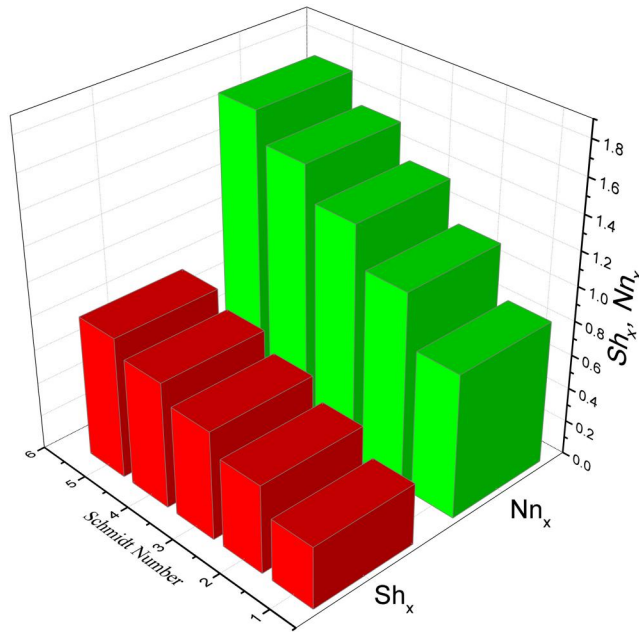


Figure 20. Impact of  $Sc$  &  $S_b$  on  $Sh_x$  &  $Nn_x$ .

well as the  $(g_1, g_2, g_3, g_4)$ . The number of terms in the rational function affects the numerical values' convergence. Choosing more terms in the power series, on the other hand, improves the precision of the result. The obtained solutions are validated by comparing them to the existing literature, which is listed in Table 2. Yacob et al. [50] used the Keller box method to obtain the solutions whereas, Dinarvand [51] used MATLAB's bvp4c package to obtain the solutions.

## 4. Results and discussion

The analysis of AA7072– deionized water flow across a wedge in the existence of microorganisms is performed using the DTM. The use of modified Buongiorno's model that discusses the impact of nanoparticle volume fraction in addition to the slip mechanisms; thermophoresis and Brownian motion helped in arriving at the more realistic model. Also the effect of nanoparticle weight is analyzed for the flow and heat transfer profiles of nanofluid. The outcomes of the study are discussed through graphs in this section. These graphs demonstrate the behavior of fluid profiles for the change in flow parameters.

The rise in the weight of the AA7072 nanoparticle suspension causes the nanofluid to become heavier and since the weight is a downward force it opposes the fluid flow and hence the velocity of fluid flow is reduced (Figure 3). This reduction in velocity allows the nanoparticle to stay at a point for a longer period so that it can conduct more heat and also the increase in  $w$  turns out to be the reason for an increased number of nanoparticles that boosts the overall thermal conductance of the nanofluid (Figure 4). The effect of the moving wedge enhances the velocity due to the fact that the positive values of  $\Lambda$  correspond to the motion of the wedge along with the free stream flow of nanofluid. This creates a force that supports the nanofluid motion along its direction hence the velocity of the fluid increases (Figure 5). The increases in the velocity of the nanofluid may not allow the nanoparticle to conduct heat to its full capacity and thus the temperature decreases with the increase in  $\Lambda$  (Figure 6). Further the increased velocity will takeaway the nanoparticles far from the boundary layer thus decreasing the nanoparticle concentration (Figure 7) and similarly, the microorganisms tend to move toward the boundary rejoin due to the concentration gradient thus leading to the enhancement in motile density at the boundary layer (Figure 8).

The slip mechanisms namely, thermophoresis and Brownian motion are experienced by the solid suspensions within the fluid and have an important role in the heat and mass transfer characteristics of the nanofluid. The metal suspensions move from hotter region to cooler region due to thermophoresis thus increasing the temperature of the nanofluid (Figure 9) and decreasing the concentration of nanoparticle (Figure 10). Similarly, the solid particles move from higher concentrated region to lower concentrated region due to Brownian motion and the increase in the values of  $Nb$  corresponds to the increased movement of nanoparticles causing an increase in the thermal profile (Figure 11) and concentration profile (Figure 12). The temperature gradient decreases between the hot surface and the surfaces away from it for an increase in thermal stratification and thus the temperature decreases (Figure 13). Similarly, the concentration gradient between these two regions of nanofluid diminishes with the increment in concentration stratification and thus a reduction in the nanoparticle concentration is observed for an increase in  $S_2$  (Figure 14).

The nanoparticle movement and microorganisms swimming within the nanofluid enhance with the increase in Schmidt number this will cause increased mass diffusivity that in turn reduces the mass concentration (Figures 15 and 16). The higher values of Peclet number causes the self-propelled microorganisms to move at a greater speed than the nanofluid. Hence, the motile density at the surface reduces (Figure 17). The rise in the wedge parameter has a greater impact on the motile density than any other fluid profile. The increase in  $\Lambda$  enhances the heat and mass transfer rates but diminishes the skin friction (Figure 18). Furthermore, as the strength of the stratification increases the heat and mass transfer rates decreases (Figure 19). The increase in Schmidt number causes more diffusion and hence the mass transfer rate increases due to its rapid movement (Figure 20).

## 5. Conclusion

The two-dimensional Heimanz laminar flow of AA7072– deionized water nanofluid past a wedge is analyzed in the existence of gyrotactic microorganisms and thermal and solutal stratification.

The flow is modeled using modified Buongiorno's heat and mass equation that includes the two major phenomena experienced by nanoparticles while moving in a fluid namely thermophoresis and Brownian motion. The model that describes this flow is transformed to a set of ordinary differential equations by using suitable transformation and the analysis is performed through DTM equipped with Padé approximant. The study's significant findings are as follows:

- The wedge parameter opposes the fluid flow and thus helps in conducting more heat.
- The concentration of microorganisms is enhanced for an increase in wedge parameter.
- The increase in the weight of nanoparticles makes the fluid heavier and hence opposes the fluid flow which results in enhanced heat conduction.
- Stratification parameters have a decreasing effect on both temperature and concentration profiles.
- The density of microorganisms decreases with bioconvection Schmidt number and Peclet number.
- The mathematical model described in this study will have a prominent role in enhancing the efficiency of thermal extrusion systems.

This study on the Heimanz flow of AA7072– deionized water has provided some valuable insights into the field of nanofluid. However, there is still much room for further exploration in this area. For instance, the studies related to choosing the optimal nanoparticle concentration help industries to synthesize the nanoparticles and use nanofluids effectively. Rheological properties can further be explored to understand the behavior of nanofluid in a much better way. The study can be explored under various other physical instances that are encountered in real life.

## Disclosure statement

No potential conflict of interest was reported by the authors.

## Funding

This work was supported by the Deanship of Scientific Research at King Khalid University through large group Research Project under grant number RGP2/230/44.

## ORCID

V. Puneeth  <http://orcid.org/0000-0003-4470-6884>

Ali J. Chamkha  <http://orcid.org/0000-0002-8335-3121>

## References

- [1] X. Li, A. U. Khan, M. R. Khan, S. Nadeem and S. U. Khan, "Oblique stagnation point flow of nanofluids over stretching/shrinking sheet with cattaneo–christov heat flux model: existence of dual solution," *Asymmetry Carbohydr.*, vol. 11, no. 9, pp. 1070, 2019. DOI: [10.3390/sym11091070](https://doi.org/10.3390/sym11091070).
- [2] M. R. Khan, K. Pan, A. U. Khan and N. Ullah, "Comparative study on heat transfer in cnts-water nanofluid over a curved surface," *Int. Commun. Heat Mass Transf.*, vol. 116, pp. 104707, 2020. DOI: [10.1016/j.icheatmasstransfer.2020.104707](https://doi.org/10.1016/j.icheatmasstransfer.2020.104707).
- [3] S. Nadeem, M. Riaz Khan and A. U. Khan, "Mhd oblique stagnation point flow of nanofluid over an oscillatory stretching/shrinking sheet: existence of dual solutions," *Phys. Scr.*, vol. 94, no. 7, pp. 075204, 2019. DOI: [10.1088/1402-4896/ab0973](https://doi.org/10.1088/1402-4896/ab0973).
- [4] D. Qaiser, Z. Zheng and M. R. Khan, "Numerical assessment of mixed convection flow of walters-b nanofluid over a stretching surface with Newtonian heating and mass transfer," *Therm. Sci. Eng. Prog.*, vol. 22, pp. 100801, 2020. DOI: [10.1016/j.tsep.2020.100801](https://doi.org/10.1016/j.tsep.2020.100801).

- [5] M. R. Khan, K. Pan, A. U. Khan and S. Nadeem, "Dual solutions for mixed convection flow of sio<sub>2</sub>- al<sub>2</sub>o<sub>3</sub>/ water hybrid nanofluid near the stagnation point over a curved surface," *Phys. A (Amsterdam, Neth)*, vol. 547, pp. 123959, 2020. DOI: [10.1016/j.physa.2019.123959](https://doi.org/10.1016/j.physa.2019.123959).
- [6] S. Nadeem, M. R. Khan and A. U. Khan, "Mhd stagnation point flow of viscous nanofluid over a curved surface," *Phys. Scr.*, vol. 94, no. 11, pp. 115207, 2019. DOI: [10.1088/1402-4896/ab1eb6](https://doi.org/10.1088/1402-4896/ab1eb6).
- [7] P. Barnoon, D. Toghraie, F. Eslami and B. Mehmandoust, "Entropy generation analysis of different nanofluid flows in the space between two concentric horizontal pipes in the presence of magnetic field: single-phase and two-phase approaches," *Comput. Math. Appl.*, vol. 77, no. 3, pp. 662–692, 2019. DOI: [10.1016/j.camwa.2018.10.005](https://doi.org/10.1016/j.camwa.2018.10.005).
- [8] K. Al-Farhany, M. A. Alomari, N. Biswas, A. Laouer, A. M. Abed and W. Sridhar, "Magneto hydrodynamic double-diffusive mixed convection in a curvilinear cavity filled with nanofluid and containing conducting fins," *Int. Commun. Heat Mass Transf.*, vol. 144, pp. 106802, 2023. DOI: [10.1016/j.icheatmasstransfer.2023.106802](https://doi.org/10.1016/j.icheatmasstransfer.2023.106802).
- [9] T. Hymavathi and W. Sridhar, "Numerical solution to mass transfer in mhd flow of Casson fluid with suction and chemical reaction," *Int. J. Chem. Sci.*, vol. 14, no. 4, pp. 2183–2197, 2016.
- [10] W. Sridhar, G. Vijaya Lakshmi, K. Al-Farhany and G. R. Ganesh, "Mhd Williamson nanofluid across a permeable medium past an extended sheet with constant and irregular thickness," *Heat Trans.*, vol. 50, no. 8, pp. 8134–8154, 2021. DOI: [10.1002/htj.22270](https://doi.org/10.1002/htj.22270).
- [11] T. Javed, A. Ghaffari and T. Hayat, "Enhancement of heat transfer in elastico-viscous fluid due to nanoparticles, where the fluid is impinging obliquely to the stretchable surface: a numerical study," *Appl. Appl. Math. Int. J.*, vol. 11, no. 1, pp. 16, 2016.
- [12] W. K. Usafzai, A. M. Saeed, E. H. Aly, V. Puneeth and I. Pop, "Wall jet nanofluid flow with thermal energy and radiation in the presence of power-law," *Numer. Heat Transf. A Appl.*, pp. 1–13, 2023. DOI: [10.1080/10407782.2023.2222456](https://doi.org/10.1080/10407782.2023.2222456).
- [13] J. Buongiorno, "Convective transport in nanofluids," *Am. J. Heat Mass Transf.*, vol. 128, no. 3, pp. 240–250, 2006.
- [14] M. Eslamian, M. Ahmed, M. El-Dosoky and M. Saghir, "Effect of thermophoresis on natural convection in a rayleigh–benard cell filled with a nanofluid," *Int. J. Heat Mass Trans.*, vol. 81, pp. 142–156, 2015. DOI: [10.1016/j.ijheatmasstransfer.2014.10.001](https://doi.org/10.1016/j.ijheatmasstransfer.2014.10.001).
- [15] M. H. Matin and B. Ghanbari, "Effects of Brownian motion and thermophoresis on the mixed convection of nanofluid in a porous channel including flow reversal," *Transp. Porous Med.*, vol. 101, no. 1, pp. 115–136, 2014. DOI: [10.1007/s11242-013-0235-x](https://doi.org/10.1007/s11242-013-0235-x).
- [16] Z. Haddad, E. Abu-Nada, H. F. Oztop and A. Mataoui, "Natural convection in nanofluids: are the thermophoresis and Brownian motion effects significant in nanofluid heat transfer enhancement," *Int. J. Therm. Sci.*, vol. 57, pp. 152–162, 2012. DOI: [10.1016/j.ijthermalsci.2012.01.016](https://doi.org/10.1016/j.ijthermalsci.2012.01.016).
- [17] P. Durgaprasad, S. Varma, M. M. Hoque and C. Raju, "Combined effects of Brownian motion and thermophoresis parameters on three-dimensional (3d) Casson nanofluid flow across the porous layers slendering sheet in a suspension of graphene nanoparticles," *Neural Comput. Applic.*, vol. 31, no. 10, pp. 6275–6286, 2019. DOI: [10.1007/s00521-018-3451-z](https://doi.org/10.1007/s00521-018-3451-z).
- [18] K. Rafique *et al.*, "Brownian motion and thermophoretic diffusion effects on micropolar type nanofluid flow with soret and dufour impacts over an inclined sheet: Keller-box simulations," *Astrophys.* vol. 12, no. 21, pp. 4191, 2019. DOI: [10.3390/en12214191](https://doi.org/10.3390/en12214191).
- [19] A. Mahmood, B. Chen and A. Ghaffari, "Hydromagnetic Hiemenz flow of micropolar fluid over a nonlinearly stretching/shrinking sheet: dual solutions by using Chebyshev spectral newton iterative scheme," *J. Magn. Magnet. Mater.*, vol. 416, pp. 329–334, 2016. DOI: [10.1016/j.jmmm.2016.05.001](https://doi.org/10.1016/j.jmmm.2016.05.001).
- [20] E. Sangeetha and P. De, "Stagnation point flow of bioconvective mhd nanofluids over Darcy Forchheimer porous medium with thermal radiation and buoyancy effect," *BioNanoSci.*, vol. 13, no. 3, pp. 1022–1035, 2023. DOI: [10.1007/s12668-023-01132-y](https://doi.org/10.1007/s12668-023-01132-y).
- [21] E. Sangeetha, P. De and R. Das, "Hall and ion effects on bioconvective maxwell nanofluid in non-darcy porous medium," *Special Top. Rev. Porous Media*, vol. 14, no. 4, pp. 1–30, 2023. DOI: [10.1615/SpecialTopicsRevPorousMedia.v14.i4.10](https://doi.org/10.1615/SpecialTopicsRevPorousMedia.v14.i4.10).
- [22] E. Sangeetha and P. De, "Bioconvective casson nanofluid flow toward stagnation point in non-darcy porous medium with buoyancy effects, chemical reaction, and thermal radiation," *Heat Trans.*, vol. 52, no. 2, pp. 1529–1551, 2023. DOI: [10.1002/htj.22753](https://doi.org/10.1002/htj.22753).
- [23] M. S. Iqbal, A. Ghaffari and I. Mustafa, "Investigation into thermophoresis and Brownian motion effects of nanoparticles on radiative heat transfer in Hiemenz flow using spectral method," *Sci. Iran.*, vol. 0, no. 0, pp. 0–0, 2019. DOI: [10.24200/sci.2019.52384.2683](https://doi.org/10.24200/sci.2019.52384.2683).
- [24] X. Xin, A. M. Saeed, F. A. M. Al-Yarimi, V. Puneeth and S. S. Narayan, "The flow analysis of Williamson nanofluid considering the Thompson and troian slip conditions at the boundary," *Numer. Heat Transf. A Appl.*, pp. 1–17, 2023. DOI: [10.1080/10407782.2023.2212922](https://doi.org/10.1080/10407782.2023.2212922).

- [25] M. I. Ur Rehman *et al.*, “Chemical reactive process of unsteady bioconvective magneto Williamson nanofluid flow across wedge with nonlinearly thermal radiation: Darcy–Forchheimer model,” *Numer. Heat Transf. B Fund.*, vol. 84, no. 4, pp. 432–448, 2023. DOI: [10.1080/10407790.2023.2211228](https://doi.org/10.1080/10407790.2023.2211228).
- [26] J. He, Q. Deng, K. Xiao and Z. Feng, “Impingement heat transfer enhancement in crossflow by a skewed twisted rib pair for simplified leading edge structure,” *Numer. Heat Transf. A Appl.*, vol. 84, no. 7, pp. 715–731, 2023. DOI: [10.1080/10407782.2022.2154724](https://doi.org/10.1080/10407782.2022.2154724).
- [27] J. N. Jamal Mohamed, V. Rathinasamy, K. Karuppan and R. Parthasarathy, “Numerical investigation of convective cooling in a rectangular vented cavity with two inlets and a hot obstacle,” *Numer. Heat Transf. A Appl.*, vol. 84, no. 7, pp. 695–714, 2023. DOI: [10.1080/10407782.2022.2154723](https://doi.org/10.1080/10407782.2022.2154723).
- [28] H. Saffari, M. Kamali, E. Vatanjoo and E. Aminian, “Theoretical investigation on microstructured hybrid surface heat transfer characteristics with Marangoni convection effect,” *Numer. Heat Transf. A Appl.*, vol. 84, no. 7, pp. 675–694, 2022. DOI: [10.1080/10407782.2022.2154085](https://doi.org/10.1080/10407782.2022.2154085).
- [29] H. Upreti, P. Bartwal, A. K. Pandey and O. Makinde, “Heat transfer assessment for au-blood nanofluid flow in Darcy–Forchheimer porous medium using induced magnetic field and Cattaneo–Christov model,” *Numer. Heat Transf. B Fund.*, pp. 1–17, 2023. DOI: [10.1080/10407790.2023.2265555](https://doi.org/10.1080/10407790.2023.2265555).
- [30] E. Sangeetha and P. De, “Gyrotactic microorganisms suspended in MHD nanofluid with activation energy and binary chemical reaction over a non-Darcian porous medium,” *Waves Random Complex Media*, pp. 1–17, 2022. DOI: [10.1080/17455030.2022.2112114](https://doi.org/10.1080/17455030.2022.2112114).
- [31] V. Puneeth, S. Manjunatha, B. J. Gireesha and R. S. R. Gorla, “Magneto convective flow of Casson nanofluid due to Stefan blowing in the presence of bio-active mixers,” *Proc. Inst. Mech. Eng. N.*, pp. 23977914211016692, 2021.
- [32] V. Puneeth, S. Manjunatha, O. Makinde and B. Gireesha, “Bioconvection of a radiating hybrid nanofluid past a thin needle in the presence of heterogeneous–homogeneous chemical reaction,” *Am. J. Heat Mass Transf.*, vol. 143, no. 4, pp. 042502, 2021.
- [33] V. Puneeth, S. Manjunatha and B. Gireesha, “Quartic autocatalysis of homogeneous and heterogeneous reactions in the bioconvective flow of radiating micropolar nanofluid between parallel plates,” *Heat Trans.*, vol. 50, no. 6, pp. 5925–5950, 2021. DOI: [10.1002/hjt.22156](https://doi.org/10.1002/hjt.22156).
- [34] Y.-M. Chu *et al.*, “Nonlinear radiative bioconvection flow of maxwell nanofluid configured by bidirectional oscillatory moving surface with heat generation phenomenon,” *Phys. Scr.*, vol. 95, no. 10, pp. 105007, 2020. DOI: [10.1088/1402-4896/abb7a9](https://doi.org/10.1088/1402-4896/abb7a9).
- [35] S. Islam *et al.*, “Mhd darcy-forchheimer flow due to gyrotactic microorganisms of casson nanoparticles over a stretched surface with convective boundary conditions,” *Phys. Scr.*, vol. 96, no. 1, pp. 015206, 2020. DOI: [10.1088/1402-4896/abc284](https://doi.org/10.1088/1402-4896/abc284).
- [36] N. S. Khan, Q. Shah and A. Sohail, “Dynamics with cattaneo-christov heat and mass flux theory of bioconvection oldroyd-b nanofluid,” *Adv. Mater., Mech. Struct. Eng. Proc. Int. Conf.*, vol. 12, no. 7, pp. 1–20, 2020.
- [37] H. Waqas, S. U. Khan, I. Tlili, M. Awais and M. S. Shadloo, “Significance of bioconvective and thermally dissipation flow of viscoelastic nanoparticles with activation energy features: novel biofuels significance,” *Symmetry*, vol. 12, no. 2, pp. 214, 2020. DOI: [10.3390/sym12020214](https://doi.org/10.3390/sym12020214).
- [38] C. S. Reddy, F. Ali, K. Al-Farhany and W. Sridhar, “Numerical analysis of gyrotactic microorganisms in mhd radiative Eyring–Powell nanofluid across a static/moving wedge with solet and dufour effects,” *ZAMM-J. Appl. Math. Mech./Zeitschrif. Angew. Math. Mech.*, vol. 102, no. 11, pp. e202100459, 2022.
- [39] I. Mustafa, S. Shahbaz, A. Ghaffari, T. Muhammad *et al.*, “Non-similar solution for a power-law fluid flow over a moving wedge,” *Alexandria Eng. J.*, vol. 75, pp. 287–296, 2023. DOI: [10.1016/j.aej.2023.05.077](https://doi.org/10.1016/j.aej.2023.05.077).
- [40] P. Lin, A. Ghaffari, Usman, “Heat and mass transfer in a steady flow of sutterby nanofluid over the surface of a stretching wedge,” *Phys. Scr.*, vol. 96, no. 6, p. 065003, 2021. DOI: [10.1088/1402-4896/abecf7](https://doi.org/10.1088/1402-4896/abecf7).
- [41] V. Puneeth *et al.*, “Stratified bioconvective jet flow of williamson nanofluid in porous medium in the presence of arrhenius activation energy,” *J. Comput. Biophys. Chem.*, vol. 22, no. 03, pp. 309–319, 2023. DOI: [10.1142/S2737416523400069](https://doi.org/10.1142/S2737416523400069).
- [42] M. Sheikholeslami, D. Ganji and M. Rashidi, “Magnetic field effect on unsteady nanofluid flow and heat transfer using Buongiorno model,” *J. Magn. Magn. Mater.*, vol. 416, pp. 164–173, 2016. DOI: [10.1016/j.jmmm.2016.05.026](https://doi.org/10.1016/j.jmmm.2016.05.026).
- [43] M. Sheikholeslami and D. Ganji, “Nanofluid hydrothermal behavior in existence of Lorentz forces considering joule heating effect,” *J. Mol. Liq.*, vol. 224, pp. 526–537, 2016. DOI: [10.1016/j.molliq.2016.10.037](https://doi.org/10.1016/j.molliq.2016.10.037).
- [44] A. Dogonchi and D. Ganji, “Convection–radiation heat transfer study of moving fin with temperature-dependent thermal conductivity, heat transfer coefficient and heat generation,” *Appl. Thermal Eng.*, vol. 103, pp. 705–712, 2016. DOI: [10.1016/j.applthermaleng.2016.04.121](https://doi.org/10.1016/j.applthermaleng.2016.04.121).
- [45] M. M. Rashidi, “The modified differential transform method for solving mhd boundary-layer equations,” *Comput. Phys. Commun.*, vol. 180, no. 11, pp. 2210–2217, 2009. DOI: [10.1016/j.cpc.2009.06.029](https://doi.org/10.1016/j.cpc.2009.06.029).

- [46] V. Puneeth, S. Manjunatha and B. J. Gireesha, “Bioconvection in buoyancy induced flow of Williamson nanofluid over a rigid plate-dtm-padé approach,” *J. Nanofluids*, vol. 9, no. 4, pp. 269–281, 2020. DOI: [10.1166/jon.2020.1760](https://doi.org/10.1166/jon.2020.1760).
- [47] A. Pedro Pablo Cárdenas and W. Ardila, “The Zhou’s method for solving the white-dwarfs equation,” *Acta Polytech. Phys. Appl. Math.*, vol. 2013, pp. 28-32, 2013.
- [48] P. P. C. Alzate, J. J. L. Salazar and C. A. R. Varela, “The Zhou’s method for solving the Euler equidimensional equation,” *Appl. Math.*, vol. 07, no. 17, pp. 2165–2173, 2016. DOI: [10.4236/am.2016.717172](https://doi.org/10.4236/am.2016.717172).
- [49] E. Erfani, M. M. Rashidi and A. B. Parsa, “The modified differential transform method for solving off-centered stagnation flow toward a rotating disc,” *Int. J. Comput. Methods*, vol. 07, no. 04, pp. 655–670, 2010. DOI: [10.1142/S0219876210002404](https://doi.org/10.1142/S0219876210002404).
- [50] N. A. Yacob, A. Ishak and I. Pop, “Falkner–skan problem for a static or moving wedge in nanofluids,” *Int. J. Ther. Sci.*, vol. 50, no. 2, pp. 133–139, 2011. DOI: [10.1016/j.ijthermalsci.2010.10.008](https://doi.org/10.1016/j.ijthermalsci.2010.10.008).
- [51] S. Dinarvand, M. N. Rostami and I. Pop, “A novel hybridity model for tio 2-cuo/water hybrid nanofluid flow over a static/moving wedge or corner,” *Sci Rep.*, vol. 9, no. 1, pp. 16290, 2019. DOI: [10.1038/s41598-019-52720-6](https://doi.org/10.1038/s41598-019-52720-6).